Signal-Processing Approaches to Risk Assessment in Coronary Artery Disease

I. A. Kakadiaris[1], S. M. O'Malley[1], M. Vavuranakis[2], S. Carlier[3], R. Metcalfe[4], C. J. Hartley[5], E. Falk[6], and M. Naghavi[7]
Department of Computer Science
University of Houston
Houston, TX, 77204, USA
http://www.cs.uh.edu

Technical Report Number UH-CS-06-09

June 27, 2006

Keywords: biomedical imaging, intravascular, ultrasound.

Abstract

Cardiovascular disease has long been the leading cause of death in developed countries and it is rapidly gaining similar status in developing countries. Sudden heart attacks remain the primary cause of death in the United States. In the year 2004 it is estimated that more than 1.4 million Americans, and more than 19 million others worldwide, experienced a life-threatening heart attack; these unpredicted attacks account for the majority of the $280 billion burden of cardiovascular diseases. Coronary artery disease (CAD) currently claims over 12.9 million American patients. In addition, CAD is the leading cause of premature, permanent disability in the U.S. labor force and accounts for about 1/5 of all disability allowances by the Social Security Administration.

[1] Dept. of Computer Science, University of Houston, TX
[2] Dept. of Cardiology, University of Athens, Greece
[3] Cardiovascular Research Foundation, New York, NY
[4] Dept. of Mechanical Engineering, University of Houston, TX
[5] Baylor College of Medicine, Houston, TX
[6] Dept. of Cardiology, University of Aarhus, Denmark
[7] Association for Eradication of Heart Attack, Houston, TX

Signal-Processing Approaches to Risk Assessment in Coronary Artery Disease

Ioannis A. Kakadiaris, Sean M. O'Malley, Manolis Vavuranakis, Stéphane Carlier, Ralph Metcalfe, Craig J. Hartley, Erling Falk, and Morteza Naghavi

Cardiovascular disease has long been the leading cause of death in developed countries and it is rapidly gaining similar status in developing countries. Sudden heart attacks remain the primary cause of death in the United States. In the year 2004 it is estimated that more than 1.4 million Americans, and more than 19 million others worldwide, experienced a life-threatening heart attack; these unpredicted attacks account for the majority of the $280 billion burden of cardiovascular diseases. Coronary artery disease (CAD) currently claims over 12.9 million American patients. In addition, CAD is the leading cause of premature, permanent disability in the U.S. labor force and accounts for about 1/5 of all disability allowances by the Social Security Administration.

CARDIOLOGY'S RECENT PARADIGM SHIFT

Coronary artery disease occurs as a result of atherosclerosis, a condition in which fatty plaques build up on the walls of the coronary arteries. If these plaques rupture, thrombosis may occur and obstruct the flow of blood to the heart, thus causing a potentially fatal heart attack. Some plaques present a particularly high risk of rupture; these are defined as *vulnerable plaques*. In the past decade, the field of cardiology has witnessed a major paradigm shift. Previously, gradually-accumulating fatty deposits and the consequent narrowing of the coronary arteries were thought to be the culprits in acute cardiac events. Today, cardiovascular specialists know that heart attacks are caused by inflammation of the coronary arteries and thrombosis-related complications of vulnerable plaques. As a result, the discovery of vulnerable plaque has the definition of a *vulnerable patient*, i.e., an individual with a high likelihood of experiencing a heart attack in the near future [1].

CARDIOVASCULAR RISK SCREENING

Atherogenesis, or the formation of plaque, starts at a very early age and takes place over many years. The classification of plaque formation is based on a timeline from the initial inflammation to the lipid-rich plaque that leads to myocardial infarction. There are 140 million Americans over the age of 35 who are at risk of a heart attack; among this population, those in the range of 45-75 years are at highest risk for loss of productive life years. About 50-60 million people in this category may not exhibit clinical evidence of the disease, and may or may not have risk factors (race, sex, family history, hyperlipidemia, hypertension, diabetes, etc.), but they are still at risk of a heart attack. Since approximately 50% of deaths relating to acute cardiac events occur in such individuals with no prior symptoms, there is an urgent need for a wide-area screening program. Toward this end, the Association for Eradication of Heart Attack (a non-profit organization based in Houston, Texas) has developed the Screening for Heart Attack

Prevention and Education (SHAPE) program, which promotes screening based on a battery of increasingly invasive tests. Emerging diagnostic tests—unavailable even a few years ago—to assess patient vulnerability factors include novel genetic and serum biomarkers such as the inflammatory marker C-reactive protein (CRP); noninvasive imaging tests such as computed tomography (CT), ultrasonography (for which relevant risk-scoring methods have been developed), and magnetic resonance (MR) imaging; and interventional catheter-based tools that allow precise, localized assessment. All of these provide unprecedented opportunities for early detection and risk stratification for potentially vulnerable patients.

But what effect in our picture of vulnerable population would broad application of these tools have? It is estimated that screening with these techniques would identify 2-3 million additional individuals with lesions in their coronary arteries that are significant enough to require intervention. However, such a screening program would generate a huge influx of raw imaging data. For a single patient, a number of multidimensional imaging datasets are collected during the screening process, with increasing levels of storage and analysis complexity (2-D, 3-D, 2-D+time, 3-D+time, etc.). Applying these techniques to all those requiring diagnostic imaging, it is apparent that the amount of data that will be produced is overwhelming. Consequently, computational tools to assist in analyses of the pathological conditions that underlie sudden cardiac events are in high demand.

INTRAVASCULAR ULTRASOUND-BASED IDENTIFICATION OF VULNERABLE PLAQUE

Detection of the vulnerable plaques, particularly the rupture-prone vulnerable plaques (which are the culprit of many heart attacks and strokes) is one of the most active areas of research in both the cardiology and biomedical imaging communities. While there exist some non-invasive technologies (mentioned earlier) that can assess plaques morphologically, to the best of our knowledge no technology currently exists to reliably characterize plaques as *vulnerable* or *non-vulnerable* in a living human. To assist with this task, invasive technologies that are currently available, or under development, include visible-light angioscopy, near-infrared optical coherence tomography, thermography, spectroscopy, and intravascular ultrasound (IVUS). Among these technologies, IVUS is a particularly attractive option as it is well-known, widely-available, has a long history of use, and is clinically-approved.

Since the mid-1990's, interest in IVUS signal processing has increased dramatically due to the emergence of frequency-domain techniques, which have enabled *in vivo* characterization of vessel and plaque tissue properties [2]. Yet in spite of its power, the major drawback of IVUS has been its inability to provide information about plaque vulnerability, i.e., an assessment of whether a plaque is stable and requires little or no treatment, or vulnerable and requires more aggressive intervention.

To address this limitation, the presence of *vasa vasorum* (VV) microvessels (shown in Fig. 1a) could be exploited. While normally these vessels simply feed larger vessels, recent evidence suggests that

VV proliferation is a strong marker of plaque inflammation, and a preceding or concomitant factor associated with plaque rupture and instability [3, 4]. As such, a technology capable of imaging VV *in vivo* would provide the clinician with a powerful indicator of plaque vulnerability. However, so far the VV could not be imaged *in vivo;* even utilizing a high-resolution intravascular technology such as IVUS, the small scale and echo-transparency of the VV typically renders them invisible.

In what follows, we introduce a novel method that enables (for the first time) IVUS detection of atherosclerotic plaque inflammation based on quantification of VV density and perfusion. This method consists of a contrast-enhanced IVUS acquisition protocol and a series of signal/image-processing techniques to detect VV in the resulting contrast-enhanced sequences.

DATA ACQUISITION

To acquire the IVUS data, we have used both a rotating single-crystal 40 MHz scanner (Boston Scientific, Inc.; Galaxy™) and a solid-state phased-array 20 MHz scanner (Volcano Therapeutics, Inc.; Invision™). For contrast we utilize Optison™: an ultrasound contrast agent composed of albumin microspheres filled with octafluoropropane gas. The IVUS catheter is advanced percutaneously, transluminally into the patient; and imaging is typically performed near a suspect region of the arterial wall. First, a baseline IVUS signal is recorded for 1-2 min ("pre-injection" period). Next, the contrast agent is injected, temporarily washing out the IVUS signal due to the echo-opacity of the lumen ("during-injection" period). Finally, IVUS signals are collected for 1-2 min ("post-injection" period), followed by the injection of normal saline to flush residual microbubbles. During these periods the IVUS catheter is not moved.

SIGNAL PROCESSING

Following acquisition, our VV detection and imaging method consists of three steps. First, the IVUS sequence is gated to eliminate gross motion artifacts. Next, the region-of-interest of the vessel is tracked with a hybrid rigid/elastic registration technique such that relative catheter/vessel motions can be eliminated and elastic wall deformations compensated for. Finally, enhancement detection is performed using difference-imaging and statistical techniques. The resulting enhancement is visualized and quantified.

Step 1: Frame Gating – In stationary-catheter IVUS studies, maintaining a fixed catheter position with regard to an anatomic point of reference is impossible in practice due to the periodic motion of the heart. Consequently, a frame gating step is performed to ensure that only a single region of vessel is imaged throughout the sequence (due to catheter drift and cardiac and respiratory motion, the catheter may periodically move along the axis of the vessel). This gating step will pull the set of frames from the

sequence associated with the region of the vessel that is imaged most frequently by the catheter. To accomplish this goal, we employ a method based on multidimensional scaling (MDS) [5]. Given the frames under analysis, $\mathrm{F}_{1..n}$, we choose a registration metric Φ, which measures the similarity between a pair of IVUS frames (e.g., normalized cross-correlation or an ultrasound-specific metric [6]). For simplicity, we will let $\Phi(\mathrm{F}_i, \mathrm{F}_j) = \Phi_{i,j}$, and denote entries in any matrix $\mathbf{A}$ by $a_{i,j}$. The terms $\Phi_{i,j}$ are organized into a symmetric matrix $\mathbf{D}$ by letting each $d_{i,j} = \Phi_{i,j}$. Depending on the properties of the registration metric, the matrix may need to be inverted and/or rescaled to conform to the properties of a dissimilarity matrix (i.e., $d_{i,i} = 0$ and $d_{i,j} \geq 0$ for $i \neq j$). Using MDS, we create a "frame-similarity" space from $\mathbf{D}$, in which each frame in the sequence is associated with a particular point; points that are near to each other in a Euclidean sense are considered similar. Most spatial clustering algorithms are capable of clustering this space into useful groups. Here, we use the *k*-means clustering algorithm. The number of clusters is chosen by a human operator who is given a visualization of several clusterings. The cluster containing the most frames is chosen for further processing.

Step 2: Contour Tracking – The result of the frame gating is a sequence that suffers only from relatively minor residual motions. These are compensated for by tracking a pair of contours throughout the sequence using a rigid registration step, followed by an elastic registration step that uses standard deformable-model techniques [7]. The area between these contours is our region of interest. The contours are initialized by a human examiner, who provides a pair of contours for the first frame in the sequence (typically the inner and outer border of the plaque).

Contour tracking provides an inner and outer contour associated with a specific region-of-interest in each IVUS frame. The region between these contours is extracted into a rectangular raster. Due to the narrowing and widening of the area between the contours, sampling will be variable along one axis of these region images, but this is irrelevant for our purposes.

Step 3: Enhancement Detection – The goal of enhancement detection is to localize and quantify the intensity changes in the IVUS image sequence due to the presence of perfused VV in the field of view of the IVUS sensor following microbubble injection. We employ difference imaging, a change-detection technique used ubiquitously in the fields of astronomy and remote sensing. Broadly speaking, difference imaging involves the comparison of an image "before" image (I_b) and "after" (I_a). For our purposes, I_b is a baseline derived by averaging all or a subset of the pre-contrast region images. The image I_a is a single post-injection region image. A difference image is produced by pixel-wise subtraction, $I_d = I_a - I_b$, with negative values set to zero. We expect this raw image to present areas of true enhancement and low-valued areas of false enhancement due to ultrasound artifacts. To account for these, grey-level

thresholding may be applied with an automatically-determined threshold; next, a Markov modeling technique may be applied to account for spatial relationships, reducing spot noise [8].

Once enhancement detection has been performed in the region-image domain, the difference image for a particular region is mapped back to the original IVUS image, where the correspondence between detected enhancement and the IVUS features may be seen.

Step 4: Quantification and Visualization of Enhancement – To quantify enhancement, a signal is produced that is composed of the average enhancement per enhanced pixel (AEPEP) in the region of interest over time (i.e., the mean grey-level of all pixels determined to be enhanced). We fit an approximating spline to the resulting AEPEP signal to highlight trends for the human observer. Results are presented as color-coded images where the unit of intensity is a percentage (%) value that is equal to an enhanced pixel's difference level divided by the maximum grey-level difference (i.e., 255).

RESULTS

We have performed *in vivo* studies in 17 human patients undergoing percutaneous coronary interventions. Due to space limitations, the analysis of one typical case is presented. Figure 2a depicts a raw difference image showing marked enhancement in the plaque region, particularly the region at 6 o'clock and from 10-12 o'clock. Thresholded difference images (Figs. 2b and 2c) exhibit the changes in enhancement over time due to microbubble passage. A magnification of an area of enhancement is shown in Figs. 3a and 3b; this highlights the difficulty of imaging the echo-transparent VV under normal circumstances. Enhancement is plotted over time in Fig. 3c for the intimo-medial/plaque region.

DISCUSSION AND FUTURE WORK

We have introduced a method that enables IVUS imaging of VV presence. Due to the inherent limitations of *in vivo* human coronary IVUS studies, we were unable to correlate our findings with histopathological evidence of VV density. However, the significant changes in the IVUS signal after microbubble passage leave no doubt as to its ability to show contrast enhancement. Knowing that almost all blood perfusion in plaques comes through VV, we hypothesize that the enhancement is related to the density of VV in the vessel wall. A comparison of our images with the micro-CT and pathology images of VV shows a conceptual agreement. A clinical discussion of our results may be found in [9] and an in-depth technical discussion in [10].

ACKNOWLEDGEMENTS

The authors would like to thank N. Dib, R. Mehran, K. Gul, C. Stefanadis, T. Papaioannou, S. Vaina, M. Drakopoulou, and I. Mitropoulos for valuable assistance. This work was supported in part by NSF Grant IIS-0431144 and a NSF Graduate

Research Fellowship (SMO). Any opinions, findings, and conclusions or recommendations expressed in this material are those of the authors and do not necessarily reflect the views of the NSF.

Authors

Ioannis A. Kakadiaris (ioannisk@uh.edu) and Sean M. O'Malley (somalley@uh.edu) are with the Computational Biomedicine Lab, Dept. of Computer Science, Univ. of Houston, Houston, TX. Manolis Vavuranakis (mvav@otenet.gr) is with the Dept. of Cardiology, Univ. of Athens, Athens, Greece. Stéphane Carlier (scarlier@crf.org) is with the Cardiovascular Research Foundation, New York, NY. Ralph Metcalfe (metcalfe@uh.edu) is with the Dept. of Mechanical Engineering, Univ. of Houston, Houston, TX. Craig J. Hartley (chartley@bcm.tmc.edu) is with the Baylor College of Medicine, Houston, TX. Erling Falk (erling.falk@ki.au.dk) is with the Dept. of Cardiology, Univ. of Aarhus, Aarhus, Denmark. Morteza Naghavi (mn2@vp.org) is with the Association for Eradication of Heart Attack, Houston, TX.

REFERENCES

[1] M. Naghavi and P. Libby et al., "From vulnerable plaque to vulnerable patient: a call for new definitions and risk assessment strategies: Parts I-II," *Circulation*, vol. 108, 2003.

[2] A. Nair, B. D. Kuban, E. M. Tuzcu, P. Schoenhagen, S. E. Nissen, and D. G. Vince, "Coronary plaque classification with intravascular ultrasound radiofrequency data analysis," *Circulation*, vol. 106, pp. 2200-2206, 2002.

[3] M. R. Hayden and S. C. Tyagi, "Vasa vasorum in plaque angiogenesis, metabolic syndrome, type 2 diabetes mellitus, and atheroscleropathy: a malignant transformation," *Cardiovasc Diabetol*, vol. 3, 2004.

[4] F. D. Kolodgie, H. K. Gold, A. P. Burke, D. R. Fowler, H. S. Kruth, D. K. Weber, A. Farb, L. J. Guerrero, M. Hayase, R. Kutys, J. Narula, A. V. Finn, and R. Virmani, "Intraplaque hemorrhage and progression of coronary atheroma," *New England J Med*, vol. 349, pp. 2316-2325, 2003.

[5] G. A. F. Seber, "Multidimensional Scaling," in *Multivariate Observations*: Wiley, 1984.

[6] B. Cohen and I. Dinstein, "New maximum likelihood motion estimation schemes for noisy ultrasound images," *Pattern Recogn*, vol. 35, pp. 455-463, 2002.

[7] D. Metaxas and I. A. Kakadiaris, "Elastically adaptive deformable models," *IEEE T Pattern Anal*, vol. 24, pp. 1310-1321, 2002.

[8] L. Bruzzone and D. F. Prieto, "Automatic analysis of the difference image for unsupervised change detection," *IEEE T Geosci Remote Sensing*, vol. 38, pp. 1171-1182, 2000.

[9] S. Carlier, I. A. Kakadiaris, N. Dib, M. Vavuranakis, C. Stefanadis, S. M. O'Malley, C. J. Hartley, R. W. Metcalfe, R. Mehran, E. Falk, K. Gul, and M. Naghavi, "Vasa vasorum imaging: A new window to the clinical detection of vulnerable atherosclerotic plaques," *Curr Atheroscler Rep*, vol. 7, pp. 164-169, 2005.

[10] S. M. O'Malley, M. Vavuranakis, M. Naghavi, and I. A. Kakadiaris, "Intravascular ultrasound-based imaging of vasa vasorum for the detection of vulnerable atherosclerotic plaque," *Proc. Int'l Conf Medical Image Computing and Computer Assisted Intervention (MICCAI)*, vol. 1, pp. 343-351, 2005.

For video illustrating vulnerable plaques and additional figures for this paper see http://www.cbl.uh.edu/CARDIA

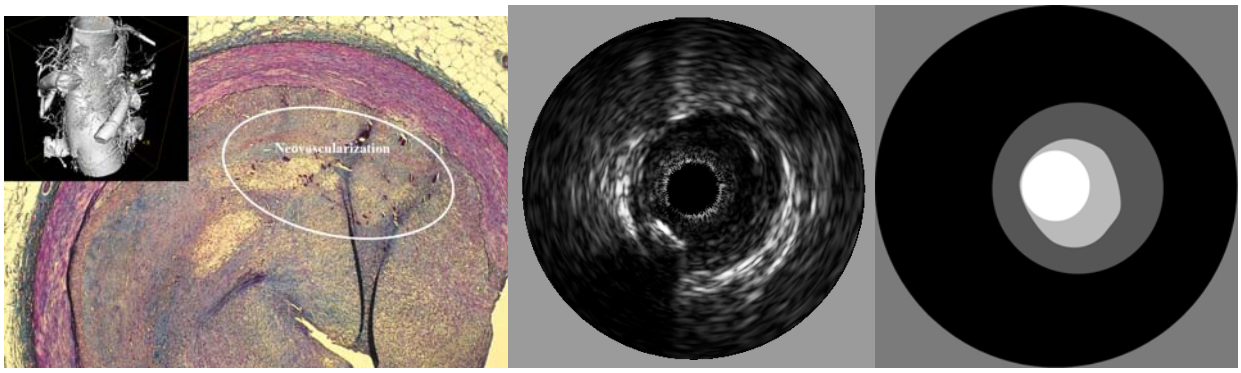

(a) (b) (c)

Figure 1: (a) Advanced atherosclerotic plaque in a hypercholesterolemic pig. Neovascularization originating from vasa vasorum is clearly seen both by histology (cross-section, circled) and micro-CT (inset, in 3-D). Cross-section may be compared to (b) a typical IVUS frame (from an unrelated case), and (c) its labeled regions. From the center outward the four regions include: the catheter; the echofree lumen; the plaque area; and the media, adventitia and surrounding tissues.

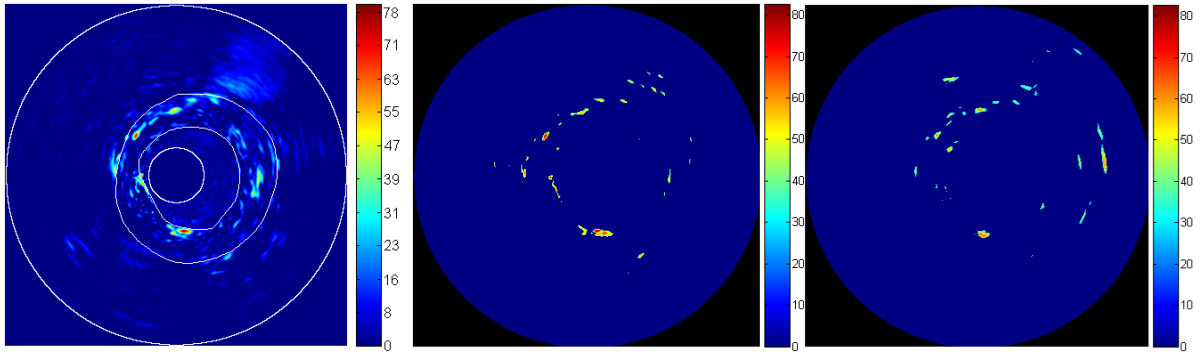

(a) (b) (c)

Figure 2: Case 1, (a) raw difference image and (b)-(c) thresholded difference images at frames 600 and 800, showing diminution over time. Unit of intensity is %, as discussed in *Step 3*.

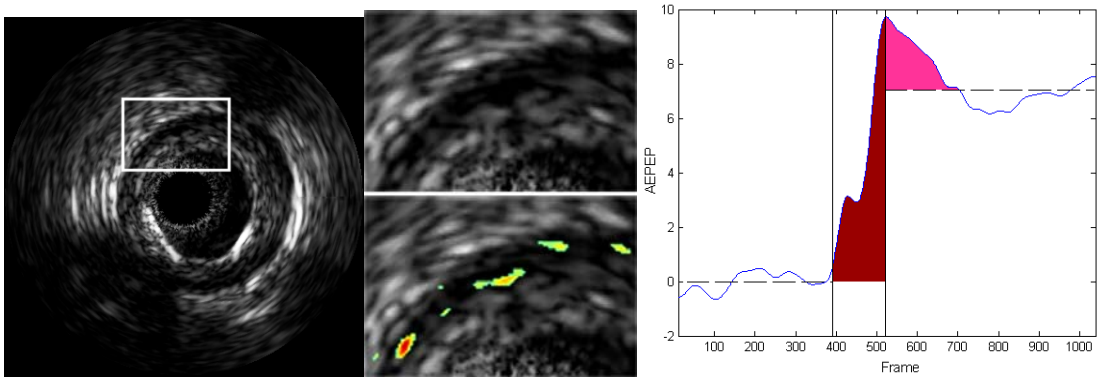

(a) (b) (c)

Figure 3: (a) Unenhanced frame from Case 1, (b) and magnified portion of frame without (top) and with (bottom) overlay showing enhanced features invisible in (a). Observe conceptual agreement with histology (Fig. 2a; note that histology is from a separate case). Enhancement is quantified over time in (c), where solid regions indicate injection period (red), return-to-baseline period (pink), and dotted lines indicate pre- and post-injection means.